First and Second Order Turbulence Closures Applied to Homogeneous Turbulent Bubbly Flows

F. Chaibina[†], G. Bellakhal and J. Chahed

University of Tunis El Manar, National Engineering School of Tunis, BP N°37, Le Belvedere, 1002 Tunis, Tunisia

†*Corresponding Author Email: fathia.chaibina@enit.utm.tn*

ABSTRACT

First and second turbulence models for turbulent bubbly flows are implemented in the CFD code. In the second order turbulence closure, the Reynolds stress tensor of the continuous phase is split into two parts: a turbulent part produced by the gradient of the mean velocity and a pseudo-turbulent part induced by the bubbles displacements; each part is predetermined by a transport equation. The turbulent viscosity issued from this modeling takes into account the excess of the agitation and the supplementary eddies stretching due to the bubbles displacements. First order turbulence closure based on this turbulent viscosity is deduced and a three-equation turbulence model (k, ks, epsilon) is developed. We present the most prominent steps of the modeling and of its implementation in the CFD code then we comment the application of the model in the two homogeneous turbulent flows (uniform and uniformly sheared bubbly flows).

Keywords: Bubbly flows; Turbulence; Pseudo turbulence; Second-order turbulence model; K-epsilon model.

NOMENCLATURE

b_{ij}	Anisotropy tensor	S_ε	inter-phase transfer of dissipation rate
C_b	Sato coefficient		
C_D	Drag coefficient	α	void fraction
d_B	bubbles diameter	δ_{ij}	Kronecker tensor
k_0	turbulent kinetic energy	ε	dissipation rate
k_s	pseudo turbulent kinetic energy	v	cinematic viscosity
R_{ij}	Reynolds Stress Tensor	v_t	turbulent viscosity
S_k	inter-phase transfer of kinetic energy	τ_b	bubbly time-scale
		τ_t	turbulent time-scale

1. INTRODUCTION

Many industrial processes involve multiphase flows. For instance, nuclear, petrochemical or environmental processes. Among them, bubbly flows are of great importance. In fact, the presence of bubbles induces a maximum of the interfacial area which enhances the mixing mechanism as well as interfacial mass transfer.

The Multiphase Computational Fluid Dynamics provides a so useful approach to simulate and design such bubbly multiphase systems. In this framework, several CFD tools are conceived for this purpose, which implies a capital importance of the adopted and implemented models in such numerical tools for turbulence closure as well as for interfacial momentum transfers.

On the other hand, countless experiments show significant modifications in two-phase bubbly flow structure. The development of two-fluid models capable to reproduce such observed changes, induced by interfacial interactions, requires adequate closures of the interfacial momentum transfer terms as well as turbulence. Moreover, many studies have proved the great influence of turbulence modeling on the prediction of the void fraction distribution: Lee *et al*. (1989), Troschko *et al.* (2001); Lance and Bataille (1991); Chahed *et al*. (2016); Rezig *et al.* (2017).

Even it was suggested by several authors Lance *et al*. (1991), Sato *et al*. (1981), Lopez *et al*. (2003) that the turbulence in gas-liquid bubbly flows comprises a "turbulent" contribution induced by shear in the liquid phase and a "pseudo-turbulent" contribution induced by the movement of the bubbles. Most turbulent models developed for bubbly flows, do not separate the two contributions and the effect of the bubbles on the turbulence of the liquid phase is introduced via additional interfacial source terms in the turbulent transport equations, Ziegenhein *et al*. (2017). We note, on the other hand, that the almost used CFD computing codes in industrial applications adopt this turbulent modeling approach.

Nevertheless, In a recent review, Risso *et al*. (2018) highlighted that turbulence models that separate the shear-induced turbulence and the bubble-induced turbulence are more likely able to take into account the effect of the bubbles on the liquid agitation, even if their use remains limited. When considering the characteristic time scales involved, such approach implies that the turbulence modeling in bubbly flow case should be founded on at least two characteristic time scales: a time scale related to the shear-induced turbulence and a time scale related to the bubble-induced turbulence.

The two-phase turbulence modeling approach of Chahed *et al*. (2003) is developed in this context. It is founded on the decomposition of the continuous phase Reynolds stress tensor in two statistically independent contributions: an irrotational (non dissipative) part induced by bubbles displacements and controlled by the added mass effect, and a turbulent (dissipative) part generated by the gradient of the mean velocity which also contains the turbulence produced in the bubbles wakes. Each part is predetermined by a transport equation. The reduction of the second order closure of the Reynolds stress tensor in bubbly flows provides an original formulation of the turbulent viscosity which involves two characteristic time scales of turbulence and pseudo turbulence.

The decomposition of the turbulence in turbulent and pseudo-turbulent contributions gives rise to two-component first and second order turbulence models. These models have been implemented in home built 2D software based on finite-difference scheme. However, this 2D software involve simplified versions of the turbulence closures which can only be applied to parallel or almost parallel 2D bubbly flows, Chahed *et al*. (2003). We present in this paper complete version of two-component first and second order turbulence models which are implemented in 3D CFD code (ANSYS CFX). The objective is to make possible the application of two-fluid models with two-component turbulence closures in the simulation of bubbly flows with complex geometries such as those used in industrial processes.

Furthermore these two-component first and second order turbulence models have been tested and validated against experimental two basic bubbly flows: uniform and uniformly sheared homogeneous turbulence. The numerical study also includes an assessment of turbulence models based on a comparison of single-component and two-component turbulence models. For this purpose, homogeneous turbulence in uniform and uniformly sheared bubbly flows represent a useful reference since the average velocities of the two phases and their volume fraction are known and the analysis can thus be focused on the capability of the turbulence models to reproduce the alteration of the turbulence structure in these two basic bubbly flows in comparison to the corresponding single-phase flows.

The comparison of single-component and two-component turbulence models makes it possible to evaluate the turbulent viscosities formulations used in first order closure of turbulence in gas-liquid bubbly flows. This would also be useful for others approaches used in the simulations of turbulent bubbly flows. For instance, Sub-Grid Scale (SGS) viscosity models used in Large Eddy Simulation (LES) of bubbly flows are in general drawn from Two-Fluid modelling based on Reynolds Averaged Navier Stokes (RANS) approach, Ma *et al*. (2015). This goes also as true for mesh-free methods such as Smoothed Particle Hydrodynamics (SPH) which appears to be well suited to gas-liquid two phase flows. The implementation of these methods in the simulation of turbulent two-phase flows requires further progress in order to develop suitable Sub-Particle Scale (SPS) turbulence models Gong *et al.* (2016).

The paper is organized as follows. Firstly we present the second and first-order turbulence models for bubbly flows as it is implemented in the original CFD code. Then, we present the second order turbulence model based on two-component closure as well as its reduction to first order turbulence model. Finally ,we present the numerical implementation and discuss the results obtained with the proposed turbulent approaches in uniform and uniformly sheared homogeneous bubbly. An assessment of turbulence models is also carried out on the basis of a comparison of single-component and two-component turbulence models applied to the simulation of homogeneous turbulence in uniform and uniformly sheared bubbly flows.

2. SECOND AND FIRST-ORDER TURBULENCE CLOSURES IN LIQUID PHASE USING ONE TIME SCALE

The turbulence closure for bubbly flows used in common CFD codes are founded upon one characteristic time scale.

2.1 Second Order Turbulence Closure

For the second-order closure, the two-phase flow version of Reynolds stress models R_{ij} adopted in

common CFD codes is similar to the single-phase version. The only difference consists on multiplying all the flux and source terms by volume fractions.

The corresponding characteristic timescale may be deduced using the following expression:

$$\tau_t^{R_{ij}} = \frac{R_{ii}}{2\varepsilon} \tag{1}$$

2.2 First Order Turbulence Closure

We start by a description of classical first-order two-equation model k-ε for bubbly flows. The turbulent kinetic energy equation and its dissipation rate ε are assumed to take a similar form as single-phase transport equations to which interfacial source terms should be added:

$$\frac{\partial}{\partial t}\left((1-\alpha)\,k\right) + \frac{\partial}{\partial x_j}\left((1-\alpha)\overline{\overline{u}}_j\,k\right) = \frac{\partial}{\partial x_j}\left((1-\alpha)\,(\frac{v_t}{\sigma_k}+v)\,\frac{\partial k}{\partial x_j}\right)$$
$$+ \ (1-\alpha)(P-\varepsilon) \ + \ S_k \tag{2}$$

$$\frac{\partial}{\partial t}\left((1-\alpha)\,\varepsilon\right) + \frac{\partial}{\partial x_j}\left((1-\alpha)\overline{\overline{u}}_j\,\varepsilon\right) = \frac{\partial}{\partial x_j}\left((1-\alpha)\,(\frac{v_t}{\sigma_\varepsilon}+v)\,\frac{\partial \varepsilon}{\partial x_j}\right)$$
$$+ \ (1-\alpha)\frac{\varepsilon}{k}(C_{\varepsilon 1}P - C_{\varepsilon 2}\,\varepsilon) \ + \ S_\varepsilon \tag{3}$$

Where:

σ_k ; σ_ε ; $C_{\varepsilon 1}$ and $C_{\varepsilon 2}$ are constants

S_k ; S_ε represents the inter-phase transfer of the kinetic energy and their dissipation rate. The interfacial source terms in the transport equation of the turbulent energy and of its dissipation rate are related to the energy produced by the drag force:

$$S_k = C_T\,\alpha\,\frac{3}{4}\frac{C_D}{d}\left|\overline{\overline{u}}_R\right|^3 \tag{4}$$

$$S_\varepsilon = C_{3\varepsilon}\,\frac{\varepsilon}{k}\,S_k \tag{5}$$

According to Lee *et al*. (1989) the coefficient

$C_T = 0.25C_D^{4/3}$ and the coefficient $C_{\varepsilon 3} = 1.92$.

The turbulent eddy viscosity is given by the following expression:

$$v_t = c_\mu\,(\frac{k^2}{\varepsilon}) \tag{6}$$

Sato *et al*. (1981) introduced a supplementary turbulent viscosity induced by bubbles:

$$v_t = \ v_{t\,m} + v_B \tag{7}$$

Where:

$v_{t\,m}$, v_B represent respectively the viscosity inherent to the liquid and the bubbly induced viscosity defined by:

$$v_B = C_b\,\alpha\,d_B\left\|\overline{\overline{U_R}}\right\| \tag{8}$$

3. SECOND AND FIRST-ORDER TURBULENCE IN LIQUID PHASE BASED ON TURBULENCE DECOMPOSITION

3.1 Second Order Closure of the Turbulence in the Liquid Phase

The second order closure of the turbulence in the liquid phase is based on the decomposition of the Reynolds stress tensor of the continuous phase into two independent components: a turbulent component $\overline{\overline{u_i'u_j'}}^{(T)}$ generated by the gradient of the mean velocity which also contains the turbulence produced in the bubbles wakes and an irrotational component $\overline{\overline{u_i'u_j'}}^{(S)}$ induced by the bubbles displacements and controlled by the added mass effects as follows:

$$\overline{\overline{u_i'u_j'}} \ = \ \overline{\overline{u_i'u_j'}}^{(T)} \ + \ \overline{\overline{u_i'u_j'}}^{(S)} \tag{9}$$

Each part is predetermined by a transport equation.

The modeling of the transport equation of the pseudo-turbulent part of the Reynolds stress tensor in the liquid phase is based on the theoretical solution in homogeneous potential flow Wijngaarden *et al*. (1984).

$$\frac{D}{Dt}\overline{\overline{u_i'u_j'}}^{(S)} \ = \ Diff \ (\overline{\overline{u_i'u_j'}}^{(S)}) + \frac{3}{20}\frac{D}{Dt}\,\alpha\left\|\overrightarrow{u_R}\right\|^2\delta_{ij}$$
$$+\frac{1}{20}\frac{D}{Dt}\,\alpha\,\overline{\overline{u}}_{Ri}\,\overline{\overline{u}}_{Rj} \tag{10}$$

With $\left\|\overrightarrow{u_R}\right\|$ is the relative velocity and α is the void fraction.

The two last terms in Eq. (10) can be explained as the contribution, in inhomogeneous flow, of the interfacial production by the added mass force $P_{ij}^{(S)}$ and of the redistribution by the pressure-strain correlation $\Phi_{ij}^{(S)}$ with:

$$\Phi_{ij}^{(S)} = \frac{3}{10}trace\,(P_{ij}^{(S)})\delta_{ij} - \frac{9}{10}P_{ij}^{(S)} \tag{11}$$

Where $P_{ij}^{(S)} = \frac{1}{2}\frac{D}{Dt}\,\overline{\overline{\alpha u_{Ri}u_{Rj}}} \tag{12}$

The pseudo-turbulent part of the energy is then deduced as the half trace of $\overline{\overline{u_i'u_j'}}^{(S)}$:

$$k_S = \frac{1}{2}\overline{\overline{u_i'u_i'}}^{(S)} \tag{13}$$

In the transport equation of the turbulent part of the Reynolds stress tensor, Eq. (14), we assume that the interfacial production of the turbulent energy and its dissipation rate are balanced in the bubbles wakes. The dissipation rate is thus identified to the

isotropic dissipation in the small scales ε_0 and computed from a similar single-phase transport equation, Eq. (15), with the characteristic timescale τ_t :

$$\overline{\overline{u_i'u_j'}}^{(T)} = Diff \, (\overline{\overline{u_i'u_j'}}^{(T)}) - (\overline{\overline{u_j'u_k'}}\frac{\partial \overline{\overline{u_i}}}{\partial x_k} + \overline{\overline{u_i'u_k'}}\frac{\partial \overline{\overline{u_i}}}{\partial x_k})$$

$$+(\Phi_{ij}^{(NL)} + \Phi_{ji}^{(NL)}) + (\Phi_{ij}^{(L)} + \Phi_{ji}^{(L)}) - \frac{2}{3}\varepsilon_0 \delta_{ij} \qquad (14)$$

$$\frac{D}{Dt}\varepsilon_0 = Diff \, (\varepsilon_0) + \frac{1}{\tau_t}(-C_{1\varepsilon}\overline{\overline{u_i'u_k'}}\frac{\partial \overline{\overline{u_i}}}{\partial x_k} - C_{2\varepsilon}\varepsilon_0)$$

$$(15)$$

The turbulent part of the energy is equally deduced as the half trace of $\overline{\overline{u_i'u_j'}}^{(T)}$:

$$k_0 = \frac{1}{2}\overline{\overline{u_i'u_i'}}^{(T)} \qquad (16)$$

With $\tau_t = \dfrac{k_0}{\varepsilon_0}$ $\qquad (17)$

The model of the redistribution terms in Eq. (18) is modified to take into account the interfacial effects: we introduce, in the non-linear part, a supplementary stretching related to the bubbles displacements with the characteristic time scale τ_b

$$\Phi_{ij}^{(NL)} + \Phi_{ji}^{(NL)} = -C_1(\tau_t^{-1} + \alpha\tau_b^{-1})$$

$$(\overline{\overline{u_i'u_j'}}^{(T)} - \frac{1}{3}\overline{\overline{u_k'u_k'}}^{(T)}\delta_{ij}) \qquad (18)$$

With $\tau_b = C_R \dfrac{d_B}{\left\|\overrightarrow{u_R}\right\|}$ $\qquad (19)$

As in single-phase according to Launder *et al.* (1975) model the linear part of the redistribution term is modeled.

$$\Phi_{ij}^{(L)} + \Phi_{ji}^{(L)} = -\gamma_1(\Pi_{ij} - \frac{2}{3}\Pi\delta_{ij}) - \gamma_2 k (\frac{\partial \overline{\overline{u_i}}}{\partial x_j} + \frac{\partial \overline{\overline{u_j}}}{\partial x_i})$$

$$-\gamma_3(D_{ij} - \frac{2}{3}D\delta_{ij}) \qquad (20)$$

where $\Pi_{ij} = -(\overline{\overline{u_j'u_k'}}\frac{\partial \overline{\overline{u_i}}}{\partial x_k} + \overline{\overline{u_i'u_k'}}\frac{\partial \overline{\overline{u_j}}}{\partial x_k})$,

$\Pi = trace(\Pi_{ij})$

and $D_{ij} = -(\overline{\overline{u_j'u_k'}}\frac{\partial \overline{\overline{u_k}}}{\partial x_i} + \overline{\overline{u_i'u_k'}}\frac{\partial \overline{\overline{u_k}}}{\partial x_j})$,

$D = trace(D_{ij})$

The diffusion terms in Eq. (10), (14) and (15) are modeled using a gradient law Eq. (21) with a diffusion coefficient which includes two effects: the turbulent diffusion $\tau_t\overline{\overline{u_k'u_l'}}^{(T)}$ expressed according to Launder model and the effect associated with the bubbles motions. This one is modeled in the

form $\tau_b\overline{\overline{u_k'u_l'}}^{(S)}$, which generalizes Sato *et al.* (1981) model.

$$Diff \, (\varphi) = \frac{C_{s\varphi}}{(1-\alpha)}\frac{\partial}{\partial x_l}\Big[(1-\alpha)(\tau_t\overline{\overline{u_i'u_j'}}^{(T)}$$

$$+\tau_b\overline{\overline{u_i'u_j'}}^{(S)})\Big]\frac{\partial \varphi}{\partial x_k} \qquad (21)$$

The constant C_R has been adjusted by Chahed *et al.*(2003) from the homogeneous turbulence experiment and fixed to 0.67. The others constants of the turbulence model have the same values currently adopted for second-order turbulence modeling of single-phase flows. The values adopted here are presented in Table (1).

Table 1 Constants of the turbulence model

C_1	γ_1	γ_2	γ_3	$C_{1\varepsilon}$	$C_{2\varepsilon}$	C_{sk}	$C_{s\varepsilon}$
1.8	0.76	0.18	0.11	1.44	1.92	0.11	0.15

3.2 First Order Closure of the Turbulence in the Liquid Phase

According to the second closure of the turbulence in two-phase bubbly flows presented above, the balance between the production and the redistribution terms in the shear stress transport equation of a linear shear flow allows to get the explicit expression of the shear stress that provides the following expression of the turbulent viscosity in bubbly flow Bellakhal *et al.* (2004):

$$\nu_t = C_{\mu 0}\frac{k_0^2}{\varepsilon_0}\frac{(1+\frac{C_{\mu b}}{C_{\mu 0}}\frac{k_S}{k_0})}{(1+\alpha\frac{\tau_t}{\tau_b})} = \nu_{t0}\frac{(1+\frac{C_{\mu b}}{C_{\mu 0}}\frac{k_S}{k_0})}{(1+\alpha\frac{\tau_t}{\tau_b})} \qquad (22)$$

Equation (22) involves a competition between two antagonist interfacial effects: a supplementary agitation and an added eddies stretching induced by bubbles displacements.

This turbulent viscosity is on the basis of the development of first-order closure of the turbulence adapted to bubbly flows. The reduction of second-order closures gives rise to a three equation turbulence model (k_0-ks-epsilon). The transport equations of k_0, ks and of the dissipation rate are modeled from second-order closures Eqs. (14), (15) and (22), this yields:

$$\frac{D}{Dt}k_0 = \frac{C_{sk}}{(1-\alpha)}\frac{\partial}{\partial x_j}\Big[(1-\alpha)(\tau_t k_0 + \tau_b k_S)\Big]\frac{\partial k_0}{\partial x_j}$$

$$+\nu_t\frac{\partial \overline{\overline{u_i}}}{\partial x_j}(\frac{\partial \overline{\overline{u_i}}}{\partial x_j} + \frac{\partial \overline{\overline{u_j}}}{\partial x_i}) - \varepsilon_0 \qquad (23)$$

$$\frac{D}{Dt}k_s = \frac{C_{sk}}{(1-\alpha)}\frac{\partial}{\partial x_j}\Big[(1-\alpha)(\tau_t k_0 + \tau_b k_S)\Big]\frac{\partial k_s}{\partial x_j}$$

$$+\frac{1}{4}\frac{D}{Dt}\alpha\left\|\overline{u_R}\right\|^2 \qquad (24)$$

$$\frac{D}{Dt}\varepsilon_0 = \frac{C_{s\varepsilon}}{(1-\alpha)}\frac{\partial}{\partial x_j}\Big[(1-\alpha)(\tau_t k_0 + \tau_b k_S)\Big]\frac{\partial \varepsilon_0}{\partial x_j}$$

$$+\frac{\varepsilon_0}{k_0}\Big[C_{1\varepsilon}\nu_t \frac{\overline{\partial u_i}}{\partial x_j}(\frac{\overline{\partial u_i}}{\partial x_j}+\frac{\overline{\partial u_j}}{\partial x_i})-C_{2\varepsilon}\varepsilon_0\Big] \tag{25}$$

Taking into account the two component second order model. The Reynolds stress tensor is thus calculated using the Boussinesq closure:

$$\overline{u'_{Li}u'_{Lj}} = \overline{u'_{Li}u'_{Lj}}^{(T)} + \overline{u'_{Li}u'_{Lj}}^{(S)} = -\nu_t(\frac{\overline{\partial u_i}}{\partial x_j}+\frac{\overline{\partial u_j}}{\partial x_i})$$

$$+\frac{2}{3}(k_S + k_0)\delta_{ij} \tag{26}$$

It should be noted that the modelling of the diffusion terms takes into account the effect of the agitation of the bubbles by an additional diffusivity associated with the time τ_b and the pseudo - turbulent component of Reynolds tensor.

4. METHODOLOGY AND NUMERICAL IMPLEMENTATION

4.1 Implementation of the Turbulence Closure in the CFD Code

Both first and second order turbulence models have been implemented in CFD code. First order turbulence closures implementation was achieved following these steps:

- The turbulent kinetic energy has been identified to turbulent part k_0 appearing in the three equations k0-ks-epsilon model. This equation is thus modified according to Eq. (23).

- The pseudo-turbulent kinetic energy k_S has been defined as a new variable the evolution of which is described by a transport equation modeled according to Eq. (24).

- The dissipation rate is identified to ε_0 and its original transport equation is modified according to equation Eq. (25)

- On the basis of the computed values of the kinetic energy contributions k_S and k_0, the dissipation rate ε_0 and the relative velocity $\|\vec{u}_R\|$, the turbulence characteristic timescales τ_0 and τ_b are calculated according to the Eqs. (17) and (19). The turbulent viscosity is thus deduced algebraically according to Eq. (22).

A similar approach is adopted for the second order closure:

- The turbulent part of the Reynolds stress tensor $\overline{u'_i u'_j}^{(T)}$ is identified to the Reynolds stress tensor in the original turbulence model. The transport equation of which is modified according to Eq. (14).

- The pseudo-turbulent component of the Reynolds stress tensor $\overline{u'_i u'_j}^{(S)}$ is introduced as a new variable computed using transport equation modeled according to Eq.(10).

- The Reynolds stress tensor is the result of adding the two components .

It should be noted that the simulations are carried out with the same parameterisation of the turbulence closure.

4.2 Homogeneous Turbulence Experiments

We note in this work turbulence models without turbulence decomposition as the "standard version" and the implemented turbulence closures that decompose the turbulence in the liquid as "modified version".

We propose to test the two versions by comparing numerical results with experimental data related to two homogenous turbulent bubbly flow cases (uniform and uniformly sheared) carried out by Lance and Bataille. (1991) and Lance *et al.* (1991). The two-phase experiments were performed in a vertical test section of 2m in length and square (450mm x 450mm). At the first of the vein is placed a grid consisting of a square mesh network 40 mm coast. The bubbles are injected uniformly from an average characteristic size of 5 mm in the section through 260 injectors of 0.8 mm internal diameter.

Homogeneous turbulence situations are characterized by a uniform void fraction and absence of the wall. They are appropriate to validate turbulence closures by comparing homogeneous turbulent bubbly flows with the corresponding single-phase flows; especially as, the authors have taken special attention in keeping the same mean liquid velocity and shear rate in both single-phase and corresponding two-phase cases.

4.3 Numerical Implementation and Simulation Program

The computational domain represents a rectangular channel similar to the experimental one. Concerning the meshing, we adopt a structured mesh for all the domain of calculations. Following many tests of sensibility study, we select the mesh from which the numerical results do not depend on the refinement (Nx=101, Ny=21, Nz=5).

The inflow and the outflow boundary conditions are adapted respectively to the left and right faces. For the other faces, we adopt symmetry boundary conditions. As we consider stationary bubbly flows, the convergence of numerical computations is supposed to be achieved when the relative differences in standard deviations of the residuals between calculated values are less than a previously selected value, chosen as 0.001%.
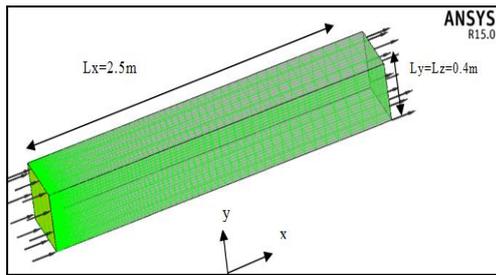
Fig. 1. Computational mesh of a uniform turbulent flow.
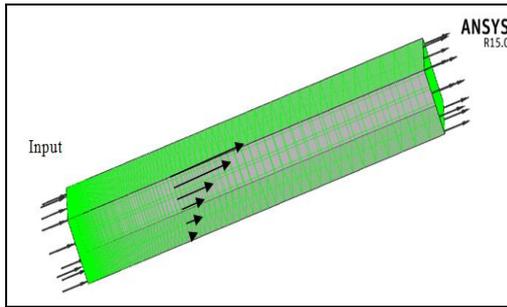
Fig. 2. Computational mesh of uniformly sheared turbulent flow (S =2.9 s⁻¹).

a) Uniform Homogeneous Turbulent Bubbly flows

In order to analyze the results of numerical simulations resulting from new turbulence closures implantation, we start with the standard version of the turbulence model applied to uniform homogeneous turbulent bubbly flows for a different void fraction (0%, 0.5%, 1%, and 2%). The effect of the coefficient of the interfacial transfer $C_{\varepsilon 3}$ has been evaluated by varying its value ($C_{\varepsilon 3}=1$, $C_{\varepsilon 3}=1.9$, $C_{\varepsilon 3}=2$). Then the same flows with the corresponding void fractions are calculated using the modified version of the turbulence model see table 2.

b. Uniformly Sheared Homogeneous Turbulent Bubbly flows.

The uniformly sheared turbulent bubbly flow is calculated for two void fractions ($\alpha=0.01$, $\alpha=0.014$) using the standard version of the turbulence model with the constants $C_{\varepsilon 3}$ and C_T proposed by Lee *et al* (1989). Similar simulations are carried out using the modified formulation of the turbulent viscosity proposed by Sato *et al*. (1981). The modified version of the turbulence model is applied to the same flow and the numerical results of the different models are compared and discussed.

A similar approach is applied in the assessment of second-order turbulence closure; we use the standard version of the R_{ij} model in the simulation of the homogeneous turbulence with uniform shear. The same flow is then simulated using the modified version of the second order turbulence model. The ensemble of simulations is summarised in table3.

Table 2 Simulations for uniform bubbly flows

Simulation Case	Void fraction (%)	Cε3	Shear rate (s-1)	T Closures	N Tools
SIM_0_1	0	*	0	First order	Standard Version
SIM_0_2	0	*	2,9	First order	Standard Version
SIM_0_3	0	*	2,9	Second order	Standard Version
SIM_1_1	0,5	1	0	First order	Standard Version
SIM_1_2	1	1	0	First order	Standard Version
SIM_1_3	2	1	0	First order	Standard Version
SIM_1_4	0,5	1,92	0	First order	Standard Version
SIM_1_5	1	1,92	0	First order	Standard Version
SIM_1_6	2	1,92	0	First order	Standard Version
SIM_1_7	0,5	2	0	First order	Standard Version
SIM_1_8	1	2	0	First order	Standard Version
SIM_1_9	2	2	0	First order	Standard Version
SIM_1_10	0,5	*	0	First order	Modified Version
SIM_1_11	1	*	0	First order	Modified Version
SIM_1_12	2	*	0	First order	Modified Version

**Table 3 Simulations for uniformly sheared bubbly flows**

Simulation Case	Void fraction (%)	CT	Shear rate (s-1)	T Closures	N Tools
SIM_2_1	1	Lee	2,9	First order	Standard Version
SIM_2_2	1,4	Lee	2,9	First order	Standard Version
SIM_2_3	1	Sato	2,9	First order	Standard Version
SIM_2_4	1,4	Sato	2,9	First order	Standard Version
SIM_2_5	1	**	2,9	First order	Modified Version
SIM_2_6	1,4	**	2,9	First order	Modified Version
SIM_2_7	1	**	2,9	Second order	Standard Version
SIM_2_8	1,4	**	2,9	Second order	Standard Version
SIM_2_9	1	**	2,9	Second order	Modified Version
SIM_2_10	1,4	**	2,9	Second order	Modified Version

As the standard and modified versions are equivalent in single-phase case, we start firstly by simulating single-phase cases (uniform and uniformly sheared: SIM_0_1, SIM_0_2, SIM_0_3). We fix the turbulence levels at the inlet where we assume isotropic turbulence structure. The values of the kinetic energy and of the dissipation rate are adjusted

in order to obtain numerical results that match with experimental data. Figures (3), (4) and (5) show satisfying concordance with experimental data. For the simulation of bubbly flows (SIM_1_1;...; SIM_2_10), we maintain the last single-phase cases adjustments for the inlet of turbulent parts. The bubbles relative velocity and the pseudo-turbulence are set equal to zero at the inlet.
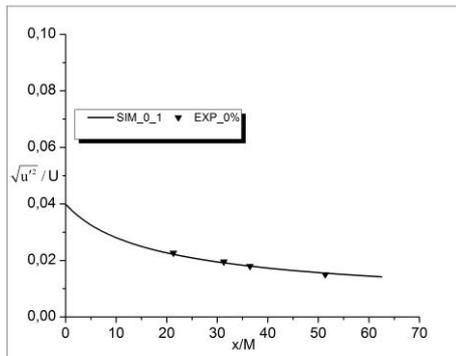
Fig. 3. Turbulent intensity $\sqrt{u'^2}/U$ behind a grid obtained by both first and second order model (U= 0.6 m/s, α= 0 %).
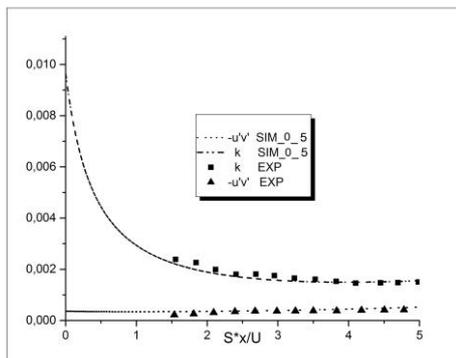
Fig.4. Decrease of the turbulent kinetic energy obtained by the first-order model (U= 1m/s, α= 0 %).
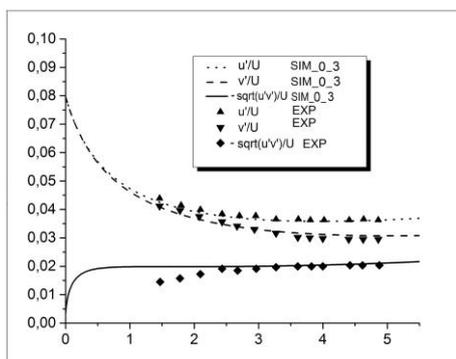
Fig. 5. Decrease of the turbulent intensity obtained by the second-order turbulence model (U= 1 m/s, α= 0 %).

5.   RESULTS AND DISCUSSION

The whole of results obtained in this work with

modified versions based on two-component turbulence models are analysed against experimental data and compared to the corresponding results obtained using the standard single-components turbulence models.

5.1. Homogeneous Bubbly flow Turbulence

The results obtained by the first order turbulence closure are the same as those obtained by the second order. Figures (6), (7) and (8) show that the standard version is incapable to reproduce the experimental data for the three void fractions (0.5 %, 1 %, 2%). In fact, with the coefficient, $C_{\varepsilon3}=1$ the model underestimates interfacial effects on the dissipation rate.by increasing its value to $C_{\varepsilon3}=1.9$, we observe a relative reduction of the turbulence but the turbulent intensity does not agree with experimental data. For $C_{\varepsilon3}=2$ we show that the turbulence is completely destroyed.
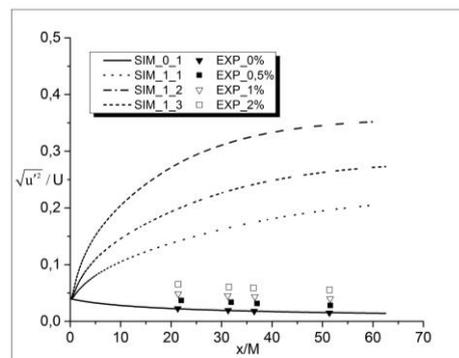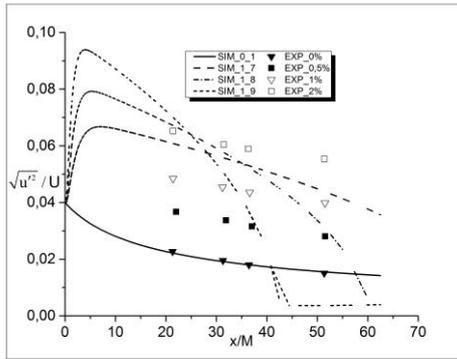

Fig. 6. Turbulent intensity $\sqrt{u'^2}/U$ behind a grid Data obtained by the standard version with $C_{\varepsilon3}=1$.
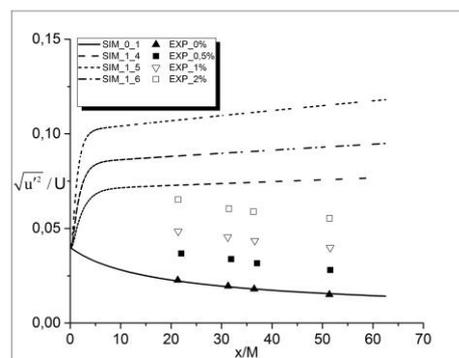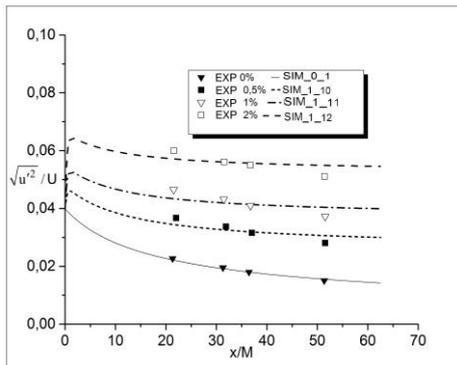

Fig. 7. Turbulent intensity $\sqrt{u'^2}/U$ behind a grid Data obtained by the standard version with $C_{\varepsilon3}=1.9$.

The numerical results of the modified version of the turbulence model are presented in (Fig.9). The results are compared to the experimental data and a good concordance is obtained. This represents a validation of the computation of the turbulent

intensity behind the grid for the one phase flow as well as the three void fractions (0.5 %; 1 %; 2%). The sleep velocity generated by the average momentum in the gas makes it possible to reproduce the interfacial turbulence so that the level of the total turbulence is correctly predicted as well as its decrease for the different void fraction.
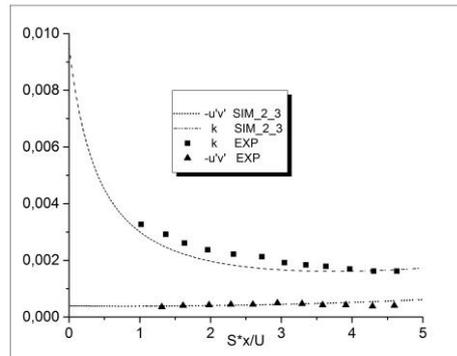
incapable to reproduce the turbulence structure. The introduction of a supplementary turbulent viscosity (Sato viscosity) does not make it possible to reduce the turbulent friction. The three equation model is based on a new formulation of the turbulent viscosity. the numerical results presented in (fig.14) and (fig.15) show a good agreement with the experimental data.
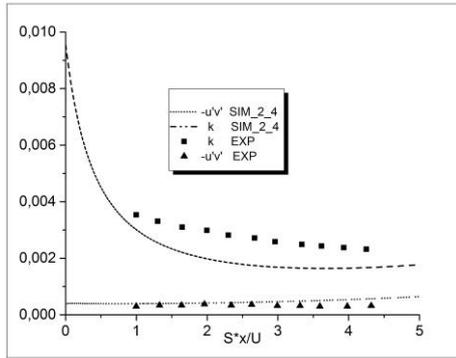

Fig. 8.Turbulent intensity $\sqrt{u'^2}$ / U **behind a grid Data obtained by the standard version with** $C_{\varepsilon 3} = 2$ **.**
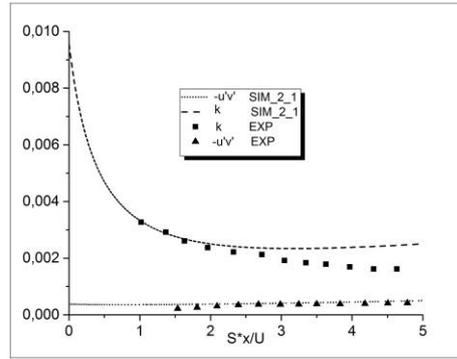
Fig. 10. Turbulent kinetic energy for α= 1 % obtained by the standard version of the turbulence model with the coefficient of Lee *et al.* (1989).

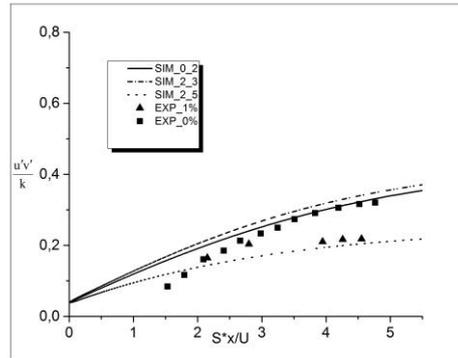**Fig. 9. Decay of the turbulent intensity** $\sqrt{u'^2}$ / U **behind a grid, obtained by the modified version.**

Fig. 11. Turbulent kinetic energy for α= 1.4 % obtained by the standard version of the turbulence model with the coefficient proposed by Lee *et al.* (1989).

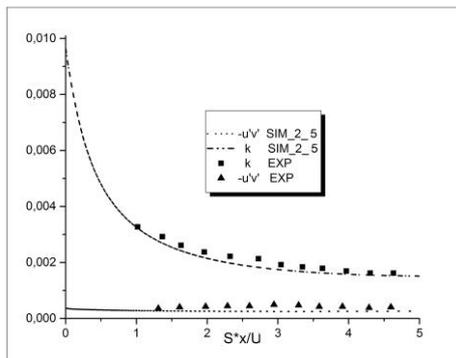## 5.2. Homogeneous Turbulence in Uniformly Sheared Bubbly flow

5.2.1. First order turbulence closure

Figures 10 and 11, present the turbulent energy obtained in the uniformly sheared bubbly flow with S=2.9 s^{-1} and for α= 0.01; α= 0.014, using the standard version of the turbulence model with the coefficient proposed by Lee *et al.* (1989). Figures 12 and 13, show the turbulent energy obtained using the standard version of the turbulence model with Sato viscosity.

In Figures. 14 and 15 we present the evolution of the turbulent kinetic energy obtained with the modified version of the turbulence model for the two void fraction α= 0.01; α= 0.014 In the bubbly flow, the standard version of the turbulence model with the interfacial source terms S_k and S_ε is

Fig. 12. Turbulent kinetic energy for α= 1 % obtained by the standard version of the turbulence model with the viscosity of Sato *et al.* (1981).
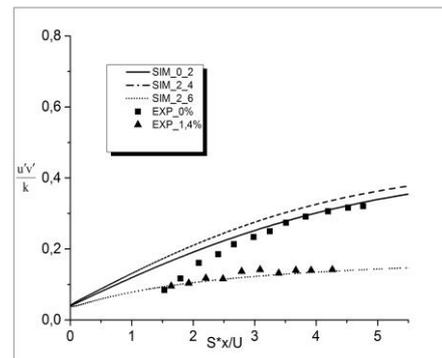
Fig. 13. Turbulent kinetic energy for α= 1.4 % obtained by the standard version of the turbulence model with the viscosity of Sato *et al.* (1981).
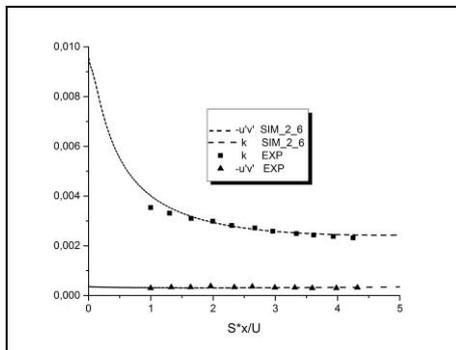

Fig. 16. Evolution of the turbulent friction normalized by the turbulent kinetic energy obtained by the three turbulence models for α= 1%.
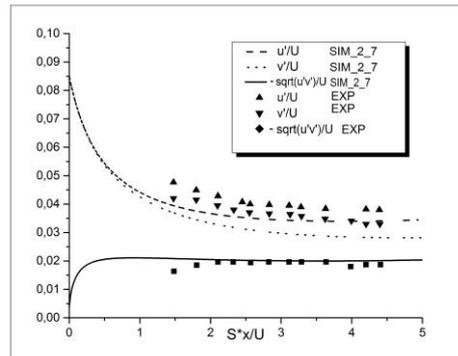

Fig. 14. Turbulent kinetic energy for α= 1% obtained by the modified version of the turbulence model.

Fig. 17. Evolution of the turbulent friction normalized by the turbulent energy obtained by the three turbulence models for α= 1.4%.

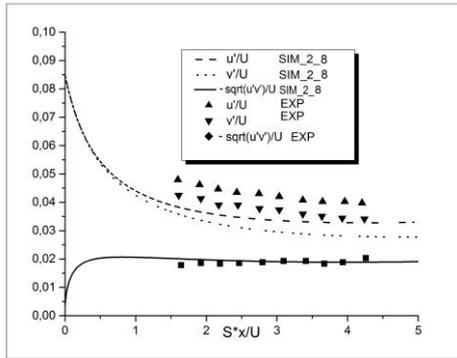**Fig. 15. Turbulent kinetic energy for α= 1.4% obtained by the modified version of the turbulence model.**

Fig. 18. Evolution of the turbulent intensity in the uniformly sheared bubbly flow for α= 0.01. Comparison between numerical results obtained by the standard version of the second order turbulence closures and experimental data.

This behavior is well demonstrated by comparing the turbulent friction normalized by the turbulent energy for the three turbulence models with experimental data for α= 0%, α= 1% and α= 1.4%, (fig. 16) and (fig.17).
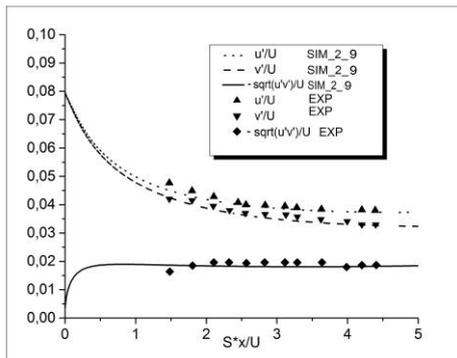
5.2.2. Second Order Turbulence Closure

Figures (18),(19),(20) and (21) show the evolution of the turbulent intensity obtained using both standard and a modified version of second-order turbulence closures for α= 0.01; α= 0.014

With uniform shear, the reduction of the turbulent shear stress indicates a diminution of the turbulent viscosity. Figures (20) and (21) present a comparison the turbulent viscosity obtained by the standard and the modified version of the turbulence closures. In addition, the modified version of the turbulence model predicts the increase of the isotropy in bubble flows, which results in a decrease in the difference between the normal Reynolds tensor components and an attenuation of the shear stress.

Fig. 19. Evolution of the turbulent intensity in the uniformly sheared bubbly flow for α= 0.014. Comparison between numerical results obtained by the standard version of the second order turbulence closures and experimental data.

Fig. 20. Evolution of the turbulent intensity in the uniformly sheared bubbly flow for α= 0.01. Comparison between numerical results obtained by the modified version of the second order turbulence closures and experimental data.
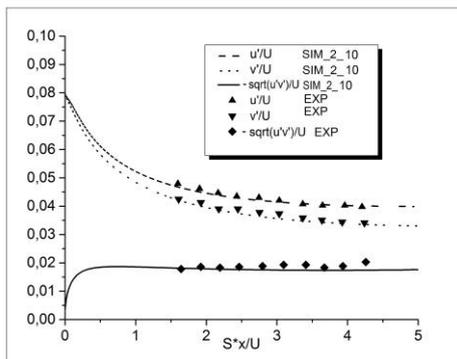
Fig. 21. Evolution of the Turbulent intensity in the uniformly sheared bubbly flow for α= 0.014. Comparison between numerical results obtained by the modified version of the second order turbulence closures and experimental data

At the production-dissipation equilibrium, we summarize in table 2 the results related to the anisotropy tensor components b_{ij} produced by the two-turbulence models in the uniformly sheared turbulent flows:

$$b_{ij} = \frac{\overline{u'_i u'_j}}{k} - \frac{2}{3}\delta_{ij} \qquad (23)$$

Table 4 Anisotropy of flow and turbulent friction at production dissipation equilibrium, comparison between the modified first and second order turbulence models with experimental data

	Void fraction %	0%	1%	1.4%
b_{l2}	Expression	-0,3	-0,2	-0,17
	Data (Lance *et al* 1990)	-0,3	-0,21	-0,15
	First order model(k-ε)	-0,3	-0,2	-0,15
	Second order model (Rij)	-0,3	-0,2	-0,15
	Sato model	-0,3	-0,32	-0,33

From table 4, we see that the two-components first and second model succeeds to reproduce the attenuation of the turbulent friction viewed in the homogeneous turbulence flows with constant shear. At production-dissipation equilibrium, the model produces lower values of turbulent eddy viscosity than those obtained in single phase flow with the same shear. This important result reflects the fact that the formulation of the turbulent viscosity keeps with the physical content of the closures developed in the second order turbulence closure so that first order three equations turbulence model k_0-k_s-ε succeeds in reproducing the modifications of the turbulence structure in bubbly homogenous turbulence uniform and with uniform shear.

6. CONCLUSION

Turbulence and pseudo-turbulence are two phenomena governed by fundamentally different mechanisms. For a moderate void fraction, these mechanisms can be described by modelling the transport equations of the Reynolds stress using scales separation. Reducing the second-order closure of turbulence provides a formulation of new turbulent viscosity that serves as a basis of the development of first-order three equation turbulence models. The numerical results of both second order and first order turbulence models succeed in reproducing both the attenuation of the turbulent friction observed in homogeneous turbulence with uniform shear and the strong increase in turbulent intensity observed in homogeneous bubbly turbulence.

Nevertheless, the turbulence model is based on a decomposition of the turbulence in turbulent dissipative and pseudo-turbulent non-dissipative

parts. The turbulent part contains the turbulence produced in the bubbles wakes which is supposed to be in equilibrium. The turbulence produced in the bubbles wakes is thus not explicitly calculated. The turbulence and pseudo-turbulence are thus arbitrary adjusted so that at the inlet the total turbulence level is well reproduced. Further progress in bubbly flows turbulence modelling could be achieved by developing specific closure for the turbulence produced in bubbles wakes especially for high void fraction bubbly flows.

REFERENCES

Bellakhel, G., J. Chahed, L. Masbernat (2004). Analysis of the turbulence statistics and anisotropy in homogeneous shear bubbly flow using a turbulent viscosity model. *Journal of Turbulence* 5, 37‑41.

Chahed, J., A. Aouadi, M. Rezig and G. Bellakhal (2016). The Phenomenon of Bubbles Negative Relative Velocity in Vertical Bubbly Jets. *Journal of Fluids Engineering* 138, 121301.

Chahed, J., V. Roig and L. Masbernat (2003). Eulerian-Eulerian two-fluid model for turbulent gas-liquid bubbly flows. *International Journal of Multiphase Flow* 29 (1), 23-49

Gong, K., S. Shao, H. Liu, B. Wang and S. K. Tan (2016). Two-phase SPH simulation of fluid–structure interactions. *Journal of Fluids and Structures* 65, 155-179.

Lance, M. and J. Bataille (1990). Turbulence in the liquid phase of a uniform bubbly air-water flow. *Journal of Fluid Mechanics* 222, 95-118.

Lance, M., J. L. Marié and J. Bataille (1991). Homogeneous turbulence in bubbly flows. *Journal of Fluids Engineering* 113, 295-300.

Launder, B. E., G. J. Reece and W. Rodi (1975).

Progress in the development of a Reynolds stress turbulence closure. *Journal of Fluid Mechanics* 68(3), 537-566.

Lee, S. J., R. T. Lahey Jr and O. C. Jones Jr (1989). The prediction of two-phase turbulence and phase distribution phenomena using k-ε model. *Japanese Journal of Multiphase Flow* 3, 335-368.

Ma, T., T. Ziegenhein, D. Lucas, E. Krepper and J. Fröhlich (2015). Euler–Euler large eddy simulations for dispersed turbulent bubbly flows. *International Journal of Heat and Fluid Flow* 56, 51-59.

Rezig, M., G. Bellakhal and J. Chahed (2017). Phase distribution in dispersed liquid-liquid flow in vertical pipe: Mean and turbulent contributions of interfacial force. *AIChE Journal* 63, 4214‑4223.

Risso, F. (2018). Agitation, mixing, and transfers induced by bubbles. *Annual Review of Fluid Mechanics*, 50, 25-48.

Sato, Y., L. Sadatomi and K. Sekouguchi (1981). Momentum and heat transfer in two-phase bubbly flow. *International Journal of Multiphase Flow* 7, 167-190.

Troshko, A. A. and Y. A. Hassan (2001). A two-equation turbulence model of turbulent bubbly flows. *International Journal of Multiphase Flow* 27, 1965‑2000.

Wijngaarden, L. Van. and A. Biesheuvel, (1984). Twophase flow equations for a dilute dispersion of gas bubbles in liquid. *Journal of Fluid Mechanics* 148, 301.

Ziegenhein, T., R. Rzehak, T. Ma and D. Lucas (2017). Towards a unified approach for modelling uniform and non-uniform bubbly flows. *The Canadian Journal of Chemical Engineering* 95, 170–79.